Numerical simulation of a triple-junction thin-film solar cell based on μc-$Si_{1-x}Ge_x$:H*

Huang Zhen-Hua(黄振华), Zhang Jian-Jun(张建军)†, Ni Jian(倪 垚), Cao Yu(曹 宇), Hu Zi-Yang (胡子阳), Li Chao(李 超), Geng Xin-Hua(耿新华), and Zhao Ying(赵 颖)

Institute of Photo-electronics Thin Film Devices and Technique, Nankai University, Tianjin 300071, *China*
Key Laboratory of Photo-electronics Thin Film Devices and Technique, Tianjin 300071, *China*
Key Laboratory of Photo-electronic Information Science and Technology of Ministry of Education, Nankai University, Tianjin 300071, *China*

(Received 1 December 2012; revised manuscript received 26 February 2013)

In this paper, a-Si:H/a-SiGe:H/μc-SiGe:H triple-junction solar cell structure is proposed. By the analyses of microelectronic and photonic structures (AMPS-1D) and our TRJ-F/TRJ-M/TRJ-B tunneling-recombination junction (TRJ) model, the most preferably combined bandgap for this structure is found to be 1.85 eV/1.50 eV/1.0 eV. Using more realistic material properties, optimized thickness combination is investigated. Along this direction, a-Si:H/a-SiGe:H/μc-SiGe:H triple cell with an initial efficiency of 12.09% (V_{oc} = 2.03 V, FF = 0.69, J_{sc} = 8.63 mA/cm^2, area = 1 cm^2) is achieved in our laboratory.

Keywords: a-Si:H/a-SiGe:H/μc-SiGe:H, triple-junction solar cell, simulation, analyses of microelectronic and photonic structures (AMPS-1D)

PACS: 88.40.jp, 88.50.gj, 71.15.Ap **DOI:** 10.1088/1674-1056/22/9/098803

1. Introduction

In order to utilize the solar spectrum efficiently for thin-film silicon solar cells, choosing the multi-junction solar cell structure is a good strategy. At present, several multi-junction structures have been proposed, such as a-Si:H/μc-Si:H, a-Si:H/a-Si:H/μc-Si:H, a-Si:H/a-SiGe:H/a-SiGe:H, a-Si:H/a-SiGe:H/μc-Si:H, and a-Si:H/μc-Si:H/μc-Si:H.[1] As for these structures, a great deal of experimental and theoretical work[2–5] has been done. As a milestone, adopting a-Si:H/a-SiGe:H/μc-Si:H configuration, Yan *et al*.[4] have attained an initial active-area cell efficiency of 16.3% with a quantum efficiency (QE) current density of about 28.6 mA/cm^2 in July 2011, which is almost close to the absorption limit of μc-Si:H solar cell if the unavoidable losses originating from the indium tin oxide (ITO) reflection and absorption, P layer absorption, and back reflector losses are taken into account. In addition, even though light trapping technologies are used, the μc-Si:H intrinsic layer is also sufficiently thick. Hence, for these structures taking μc-Si:H as the absorber of the bottom cell, weak absorption coefficient and limited absorption become the bottleneck. As a solution to this problem, μc-$Si_{1-x}Ge_x$:H alloys have been proposed as the absorber of the bottom cell by Kondo *et al*.,[6] which have been proved to possess high absorption coefficients in the whole solar spectrum compared with μc-Si:H and have a tunable bandgap in a range from 0.67 V to 1.1 V as the ratio of Ge to Si changes, and therefore it could extend the absorption scope into a longer wavelength region. Recently, they have obtained an initial efficiency of 11.6% in a structure of a-Si:H/μc-Si:H/μc-$Si_{0.9}Ge_{0.1}$:H.[7] However, in their triple-junction solar cell structure, the middle cell is fixed as μc-Si:H, which will restrict the potential of the bandgap combination. As a consequence, our group proposes a new kind of triple-junction structure: a-Si:H/a-SiGe:H/μc-SiGe:H, in which we can find the preferred bandgap configuration by modulating the bandgaps of the middle and bottom cells and achieve better utilization of the solar spectroscopy.

In this paper, at first a method of numerical simulation is employed to investigate the optimization bandgap of the a-Si:H/a-SiGe:H/μc-SiGe:H triple-junction solar cell structure based on our previous studies[8–10] on μc-SiGe:H material. In the second part, more realistic material properties are taken into account and the suitable thickness combination is studied. Finally, the experimental result following the simulation direction is presented and discussed.

2. Experiment details

The simulator adopted in this paper is the analyses of microelectronic and photonic structures (AMPS-1D)[11] which is developed by the group from the Pennsylvania State University. It can calculate solar cell parameters such as conversion efficiency (η), short circuit current (J_{sc}), open circuit voltage (V_{oc}), fill factor (FF), and internal information including carrier recombination profile and electrical field distribution, by

*Project supported by the National Basic Research Program of China (Grant Nos. 2011CBA00705, 2011CBA00706, and 2011CBA00707), the Natural Science Foundation of Tianjin City, China (Grant No. 12JCQNJC01000), and the Fundamental Research Funds for the Central Universities of China (Grant No. 65012371).

†Corresponding author. E-mail: jjzhang@nankai.edu.cn

© 2013 Chinese Physical Society and IOP Publishing Ltd

solving Poisson's equation and continuity equations for electrons and holes. The structure of the calculated triple-junction solar cell is glass/SnO_2/p1/i1/n1/p2/i2/n2/p3/i3/n3/Al, and the typical band structure in thermodynamic equilibrium is shown in Fig. 1.

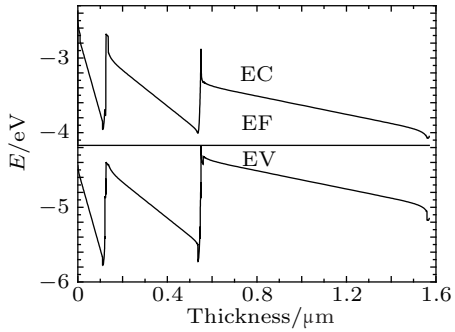


Fig. 1. Energy band structure of a-Si:H/a-SiGe:H/μc-SiGe:H triple-junction solar cell in thermodynamic equilibrium.

In the optical aspect, the absorption coefficients of the intrinsic layers with different bandgaps (a-Si:H, a-SiGe:H, μc-Si:H, μc-SiGe:H) are obtained experimentally. Losses originating from the reflection on the front surfaces and from the absorption on the front glass/SnO_2 layer are assumed to be 10%, so we set the 'light-x' parameter to be 0.90. As for the back electrode, a reflection coefficient is set to be 0.8 and other light trapping structures are not considered. In the electrical aspect, the thicknesses of all the p and n layers are fixed at 10 nm. The ubiquitous bandtail properties are also taken into account, and the characteristic energies of conduction and valence band tails for all the p and n layers are conservatively set to be 0.03 eV and 0.03 eV,[12,13] respectively. These two energies for the a-Si:H intrinsic layer are fixed at 0.025 eV and 0.05 eV,[14] and these for microcrystalline intrinsic layer are neglected. The gap states for all the intrinsic layers are described in later simulation. In addition, we chose conservative and constant values for the electron and hole mobilities of all layers, which are 20 $cm^2 \cdot v^{-1} \cdot s^{-1}$ and 2 $cm^2 \cdot v^{-1} \cdot s^{-1}$,[24] respectively. In the experimental aspect, the a-Si:H/a-SiGe:H/μc-SiGe:H triple-junction solar cells are deposited in an in-line seven-chamber RF-PECVD system,[15] and the structure of the total cell is Glass/SnO_2:F/p-a-SiC:H/i-a-Si:H/n-a-Si:H/n-μc-Si:/p-μc-Si:H/i-a-SiGe:H/n-μc-Si:H/p-μc-Si:H/i-μc-SiGe/n-a-Si/ZnO/Ag. The effective area of the cell is 1 cm^2, and the J–V characteristics are tested at 25 °C under AM1.5 100 mW/cm^2.

3. Results and discussion

3.1. TRJ-F/TRJ-M/TRJ-B tunnel-recombination junction

In order to take the triple-junction solar cell in the stacked structure as a complete single device in simulation, the tunnel-recombination junction (TRJ) which connects two p–i–n sub-cells and determines the carrier exchange is very significant. Up to now, different models have been proposed by several research groups: the trap-assisted tunnel model[5,16] from the Delft University, the low bandgap and high defective model[12,17] from the INTEC and the Utretcht University, and Yunaz's model[18,19] from the Tokyo Institute of Technology which combines some improvements of the former two models. Based on Yunaz's model, in our model a TRJ-F/TRJ-M/TRJ-B (TRJ-front/TRJ-middle/TRJ-bottom) triple structure was adopted to describe the TRJ. The schematic diagram is shown in Fig. 2. Along the direction from the TRJ-F layer to the TRJ-B layer, a grading of the mobility gap exists, which is used for the steady transition of bandgaps from the n layer of the top sub-cell (N1) to the p layer of the bottom sub-cell (P2). Besides, in the same direction, different donor-like and acceptor-like Gauss gap state density profiles are assigned, aiming to form different electron and hole recombination gradients, further to make electrons from the N1 layer and holes from the P2 layer completely exchange in several nanometers' region, and to form an ideal ohmic contact between two contiguous sub-cells.

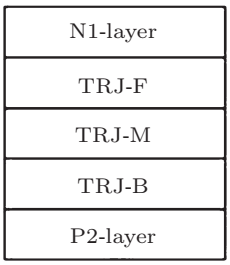


Fig. 2. Schematic diagram of the TRJ-F/TRJ-M/TRJ-B TRJ model.

These three layers are 1 nm in thick, of which the carrier mobility is set to be 10000 $cm^2/V \cdot s^{-1}$ in order to further ensure the carrier recombination in this region. The bandgap grading is 1.7 eV/1.1 eV/1.7 eV. The donor-like Gauss gap state density profile is 1×10^{15} $cm^{-3}/5 \times 10^{21}$ $cm^{-3}/1 \times 10^{20}$ cm^{-3}, and the acceptor-like Gauss gap state density profile is 1×10^{15} $cm^{-3}/5 \times 10^{21}$ $cm^{-3}/5 \times 10^{21}$ cm^{-3}. As shown in Fig. 3, the recombination is centred in the TRJ-M region and the electron current in the N1 region changes smoothly into the hole current in the P2 region. Figure 4 shows the J–V characteristics of the P/TRJ/N and PN structure, and the calculated differential resistant for the P/TRJ/N structure is found to be around 4×10^{-3} Ω/cm^2, so it illustrates that with the TRJ inserted, the PN junction changes from an ideal diode into an ideal ohmic resistant. Hence, it indicates that the TRJ-F/TRJ-M/TRJ-B model is suitable for the calculation of multi-junction solar cells.

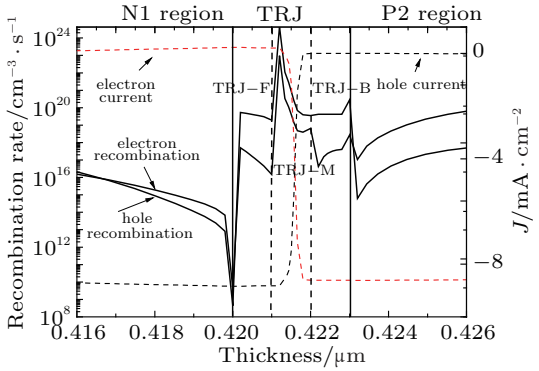


Fig. 3. (color online) Recombination distribution and the current profile in the N1/TRJ/P2 structure.

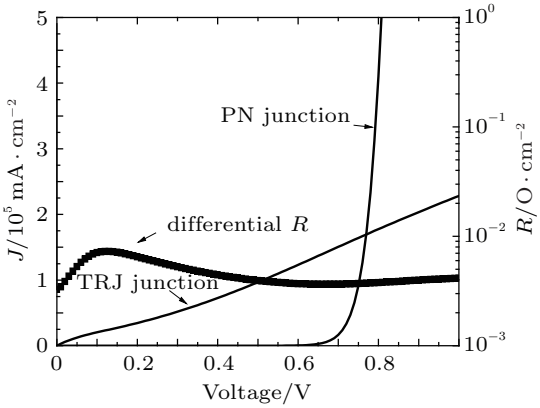


Fig. 4. The *J*–*V* characteristics of P/TRJ/N and PN structure.

3.2. a-Si:H/a-SiGe:H/uc-SiGe:H optimized bandgap combination

Based on our proposed TRJ model, we first investigate the preferred bandgap configuration in the a-Si:H/a-SiGe:H/μc-SiGe:H structure. The intrinsic layer of the top cell is fixed as a-Si:H and its bandgap is set to be 1.85 eV,[14,15] for it has been widely used in industry and multi-junction structures as a top absorption material. The bandgaps of the middle and bottom cells are varied and the thickness values of all intrinsic layers (i-top, i-middle, i-bottom) for each bandgap combination are also changed, and the ranges of the bandgap and thickness are listed in Table 1. In this calculation we just simply assume the gap state to be of uniform distribution and its value is 10^{15} cm^{-3}.[18,19] The calculated contour maps of the convention efficiency as a function of the bandgap of the middle and bottom cells are shown in Fig. 5.

Table 1. Energy band structure of a-Si:H/a-SiGe:H/μc-SiGe:H triple-junction solar cell in thermodynamic equilibrium.

	i-top	i-middle	i-bottom
Bandgap/eV	1.85	1.7–1.3	1.1–0.7
Thickness/nm	40–500	100–1000	100–6000

As Fig. 5 shows, the high efficiency appears in the area where the i-middle bandgap is located in a range of 1.46–1.51 eV and the i-bottom bandgap is located in a range of 0.97–1.01 eV. We also find that the highest efficiency of 18.56% (J_{sc} = 10.12 mA/cm^2, V_{oc} = 2.21 V, FF = 0.83) is achieved with a combination of a 1.85-eV intrinsic layer at the top, 1.5 eV in the middle, and 1.0 eV in the bottom. Thickness values of the i-top, i-middle, and i-bottom layers (t_{i-top}, $t_{i-middle}$, $t_{i-bottom}$) for the optimized triple-junction solar cell are 300, 400, and 2000 nm, respectively. The open-circuit voltages for the top, middle, and bottom cells are 1.01, 0.72, and 0.48 V, respectively. For comparison, the best efficiency for the a-Si:H/a-SiGe:H/μc-Si:H triple structure is calculated to be 17.09% (J_{sc} = 9.72 mA/cm^2, V_{oc} = 2.24 V, FF = 0.785), which is lower than those predicted by other groups,[19,21] and it is close to the best efficiency recently attained by Yan's group.[4] This is probably because that we have taken the optical losses and ubiquitous properties of Si-based material into account. According to Meillaud *et al.*'s result,[20] the relation between the energy gap and the germanium content prepared by a PECVD process exhibits an almost straight line, and a SiGe material with a bandgap of 1 eV could be achieved with 20% germanium alloy. Matsui *et al.*[21] have also proved that a good SiGe material could be obtained when the Ge content was around 20%, and reached a V_{oc} of 0.427 V under this condition. With further optimization, it is believed that a $Si_{0.8}Ge_{0.2}$:H sub-cell with a higher V_{oc} is to be expected. Thus, the best bandgap configuration of 1.85 eV/1.5 eV/1.0 eV is very charming and realizable. According to the above result, it is clear that taking the μc-SiGe:H as the bottom absorber layer and combining a middle cell with a suitable bandgap is a better choice to reach higher utilization of the solar spectrum.

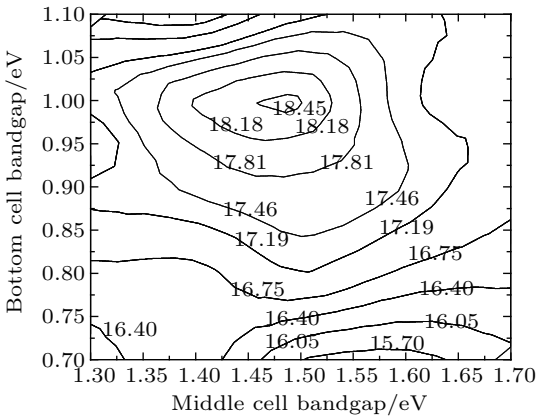


Fig. 5. Contour map of the conversion efficiency as a function of the bandgaps of the middle and bottom cells.

3.3. a-Si:H/a-SiGe:H/uc-SiGe:H thickness combination

Based on the above optimized bandgap configuration, we further consider more nonideal properties of each intrinsic layer, namely, the gap state structures of a-Si:H, a-SiGe:H, and μc-SiGe:H materials, and investigate the suitable thickness combination under this condition. The defect pool model is chosen and the densities of dangling bonds of a-Si:H and

a-SiGe:H are set to be 5×10^{15} cm^{-3} and 5×10^{16} cm^{-3},[14,22] respectively, which are thought to be the experimental values for good-quality a-Si:H and a-SiGe:H materials. The correlation energy is set to be 0.2 eV,[13,22] and other parameters can be found in the literature.[25–27] The dangling bond of the μc-SiGe:H is set to be 6×10^{15} cm^{-3}, which is a suitable value that is larger than the value used for μc-Si:H[13] and lower than the value tested by the AIST group by ESR.[28] In view of high absorption coefficient of μc-SiGe:H, $t_{\mathrm{i-bottom}}$ is fixed at 1200 nm, and in our calculation $t_{\mathrm{i-top}}$ varies from 40 nm to 500 nm and $t_{\mathrm{i-middle}}$ varies from 100 nm to 500 nm. The contour maps of the conversation efficiency, short-circuit current density, fill factor, and open-circuit voltage as a function of $t_{\mathrm{i-top}}$ and $t_{\mathrm{i-middle}}$ are shown in Fig. 6.

Several results can be extracted from Fig. 6. 1) The best efficiency can be achieved when $t_{\mathrm{i-top}}$ and $t_{\mathrm{i-middle}}$ are around 120 and 350 nm, respectively. 2) When $t_{\mathrm{i-top}}$ is from around 120 to 180 nm, and $t_{\mathrm{i-middle}}$ is between 350 nm and 450 nm, the currents of sub-cells match well (D region as shown in Fig. 6(b)). However, when the thickness configuration is located in regions A, B, and C, the total current will be restricted by the top, middle, and bottom sub-cells, respectively. 3) When $t_{\mathrm{i-top}}$ is less than 120 nm, the FF falls mainly as $t_{\mathrm{i-middle}}$ increases, but when $t_{\mathrm{i-top}}$ is over 120 nm, the FF falls apparently as $t_{\mathrm{i-middle}}$ increases. 4) The V_{oc} ranges from 2.00 to 2.08 V, and decreases slightly as $t_{\mathrm{i-top}}$ and $t_{\mathrm{i-middle}}$ increase. Furthermore, we calculate the average values of field intensity (E) in the i-top, i-middle, and i-bottom layer ($E_{\mathrm{i-top}}$, $E_{\mathrm{i-middle}}$, $E_{\mathrm{i-bottom}}$) for different thickness combinations, and the results are shown in Fig. 7. It is found that the dominant E in the triple solar cell changes as $t_{\mathrm{i-top}}$ and $t_{\mathrm{i-middle}}$ vary, and it behaves in a manner similar to the FF. For the case that $t_{\mathrm{i-top}}$ is around 120 nm, $E_{\mathrm{i-middle}}$ is dominant and drops as $t_{\mathrm{i-middle}}$ increases when $t_{\mathrm{i-middle}}$ is less than 300 nm, but then $E_{\mathrm{i-top}}$ surpasses $E_{\mathrm{i-middle}}$ and almost keeps constant as $t_{\mathrm{i-middle}}$ grows. Accordingly, the FF first declines sharply as $t_{\mathrm{i-middle}}$ grows, and then remains constant when $t_{\mathrm{i-middle}}$ is larger than 300 nm, as shown in Fig. 6(c). Thus, the FF of the triple solar cell is mainly determined by the dominant E. In contrast, the V_{oc} is determined by all the three average field intensities together, because the V_{oc} is approximately equal to the sum of the open circuit voltages of sub-cells, and the latter is basically determined by its average field intensity. The increase in $t_{\mathrm{i-top}}$ and $t_{\mathrm{i-middle}}$ induces $E_{\mathrm{i-top}}$ and $E_{\mathrm{i-middle}}$ to decrease monotonically, as shown in Fig. 7, and finally leads to the result mentioned above. On the whole, the similarity of Fig. 6(a) to Fig. 6(b) implies that the final efficiency is mostly determined by the current match state. Since in our simulation the optical scattering of SnO_2/Si interface is neglected, the actual best thickness combination will deviate from our simulation value. However, as a guide of the experimental deposition of triple-junction cells, the routine from A to D is suitable for finding the actual optimal point, namely, we should keep the current restricted by the top cell and gradually increase $t_{\mathrm{i-top}}$ to reach the current match point.

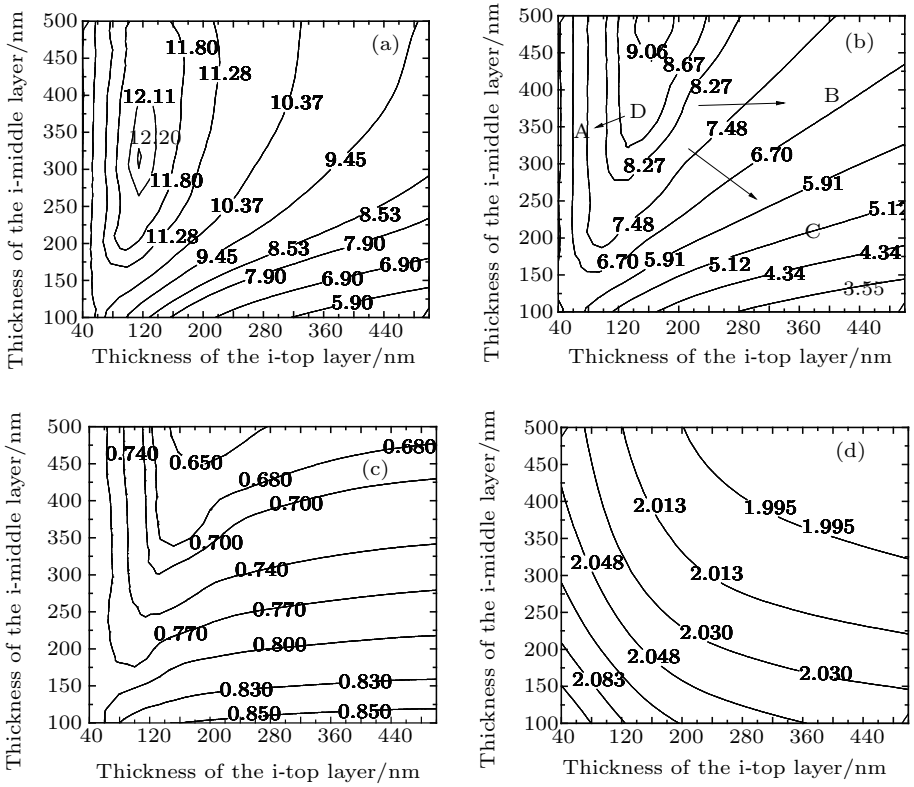


Fig. 6. Contour maps of performance parameters (a) η, (b) J_{sc}, (c) FF, and (d) V_{oc}, as a function of $t_{\mathrm{i-top}}$.

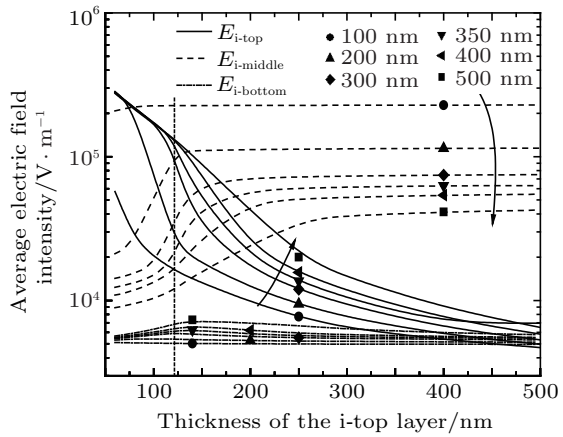


Fig. 7. Average values of field intensity (E) in the i-top, i-middle, and i-bottom layer ($E_{\text{i-top}}$, $E_{\text{i-middle}}$, $E_{\text{i-bottom}}$) for different thickness combinations. Solid, dashed, and dash-dotted lines denote $E_{\text{i-top}}$, $E_{\text{i-middle}}$, and $E_{\text{i-bottom}}$, respectively. Solid circles, up triangles, diamonds, down triangles, left triangles, and squares denote i-middle thickness values of 100, 200, 300, 350, 400, and 500 nm, respectively.

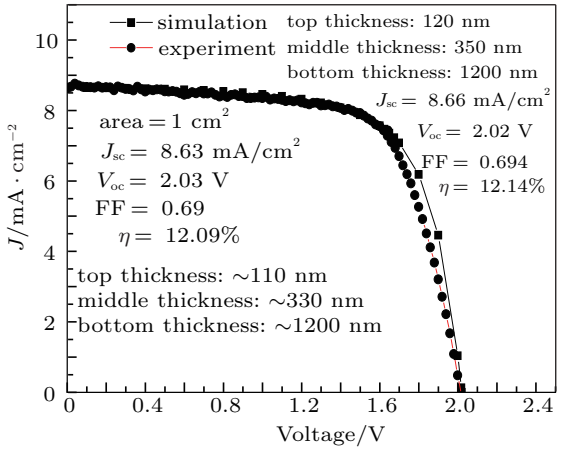


Fig. 8. (color online) J–V characteristics for a-Si:H /a-SiGe:H/μc-SiGe:H solar cell. The results of experiment and simulation are represented by solid circles and squares, respectively.

The details of optimization will be reported elsewhere, and here we present a series of results of triple-junction cells with different values of $t_{\text{i-top}}$, as shown in Table 2. By varying the deposition time, we fix $t_{\text{i-top}}$ and $t_{\text{i-bottom}}$ at around 300–350 nm and 1200–1300 nm, respectively, and change $t_{\text{i-top}}$ from 60 to 130 nm (S1 to S5 in Table 2). It is obvious that the current shows an increasing trend as $t_{\text{i-top}}$ increases, and it demonstrates that the thickness combination obtained from simulation is useful and guidable. Simultaneously, it could be found that the V_{oc} and the FF fall more quickly than simulation results, which may be attributed to the interface recombination. Thus, with finer optimization and with better TCO, we obtain an efficiency of 12.09% in the a-Si:H/a-SiGe:H/μc-SiGe:H structure, as shown in Fig. 8. We can find that the calculated FF is bigger than the actual FF, which implies that better interface optimization is still needed. At the same time, it can be seen that the actual thickness values of the i-top, i-middle, and i-bottom layer are thinner than the thickness values used in the simulation. The main reason is the ignorance of the scattering effect of SnO_2 and the back reflector as mentioned above. Even though the actual efficiency is almost close to the simulation result, it is still far from the best efficiency of 18.56% calculated in Section 3.2. As a result, the material qualities of μc-SiGe:H and a-SiGe:H need to be improved further, and the density of dangling bond requires to be lowered towards 10^{15} cm^{-3} to make the efficiency enhanced. Besides, the work mainly focuses on the bandgap configuration, and the efficiency could be enhanced further if antireflective layers novel interlayers, and other three-dimensional light trapping structures are taken into consideration in calculation. These will be discussed in detail in our future work theoretically and experimentally.

Table 2. Results of the a-Si:H/a-SiGe:H/μc-SiGe:H solar cell with different values of $t_{\text{i-top}}$.

	$t_{\text{i-top}}$/nm	J_{sc}/mA·cm^{-2}	V_{oc}/V	FF	η/%
S1	60	6.450	2.003	0.731	9.46
S2	80	6.907	2.000	0.723	9.99
S3	100	7.385	1.996	0.720	10.60
S4	120	7.833	1.979	0.706	10.90
S5	130	8.032	1.955	0.702	11.02

4. Conclusions

In this article, we have simulated the a-Si:H/a-SiGe:H/μc-SiGe:H triple junction thin-film silicon solar cell under an AMPS environment. First, we built a TRJ-F/TRJ-M/TRJ-B tunnel-recombination junction model, which is used to simulate the triple cell as a single device. We find that suitable donor-like and acceptor-like Gauss gap state density profiles are essential for the TRJ junction to behave like an ohmic contact. Secondly, we calculate the parameters of the preferred bandgap configuration for the triple-junction solar cell under ideal conditions, and they are found to be 1.85 eV in the top, 1.5 eV in the middle, and 1 eV in the bottom. This result demonstrates that better harvest of sunlight could be achieved by this structure than by traditional a-Si:H/a-SiGe:H/μc-Si:H triple structure. Thirdly, we consider more realistic material properties, and investigate the optimal thickness combination. The calculated result shows a suitable way to reach the best efficiency in our experimental optimization, along which we finally achieve an a-Si:H/a-SiGe:H/μc-SiGe:H triple cell with an initial efficiency of 12.09% ($V_{\text{oc}} = 2.03$ V, FF = 0.69, $J_{\text{sc}} = 8.63$ mA/cm^2, area =1 cm^2). This work has offered a good direction for the experiment.

References

[1] Green M, Emery K, Hishikawa Y and Warta W 2011 *Prog. Photovolt.: Res. Appl.* **19** 84

[2] Zheng X X, Zhang X D, Yang S S, Wang G H, Xu S Z, Wei C C, Sun J, Geng X H, Xiong S Z and Zhao Y 2011 *Acta Phys. Sin.* **60** 068801 (in Chinese)

[3] Yan B, Yue G, Xu X, Yang J and Guha S 2010 *Phys. Stat. Sol. A* **207** 671

[4] Yan B, Yue G, Sivec L, Yang J and Guha S 2011 *Appl. Phys. Lett.* **99** 113512

[5] Zeman M and Krc J 2008 *J. Mater. Res.* **23** 889

[6] Ganguly G, Ikeda T, Nishimiya T, Saitoh K, Kondo M and Matsuda A 1996 *Appl. Phys. Lett.* **69** 4224

[7] Matsui T, Haijun J, Kondo M, Mizuno K, Tsuruga S, Sakai S and Takeuchi Y 2010 *35th IEEE Photovoltaic Specialists Conference*, June 20–25, 2010 Hawaii, USA, p. 311

[8] Zhang L P, Zhang J J, Shang Z R, Hu Z X, Geng X H and Zhao Y 2008 *Chin. Phys. B* **17** 3448

[9] Zhang L P, Zhang J J, Zhang X, Shang Z R, Hu Z X, Zhang Y P, Geng X H and Zhao Y 2008 *Acta Phys. Sin.* **57** 7338 (in Chinese)

[10] Zhang L P 2009 *Investigation of Microcrystalline Silicon Germanium Growth and its Preliminary Application on the Solar Cells* (Ph.D. Thesis) (Tianjin: Nankai University) (in Chinese)

[11] Arch J K, Rubinelli F A, Hou J Y and Fonash S J 1991 *J. Appl. Phys.* **69** 7057

[12] Rubinelli F, Rath J and Schropp R 2001 *J. Appl. Phys.* **89** 4010

[13] Ding K, Kirchartz T, Pieters B, Ulbrich C, Ermes A, Schicho S, Lambertz A, Carius R and Rau U 2011 *Sol. Energy Mater. Sol. Cells* **95** 3318

[14] Shah A 2010 *Thin-Film Silicon Solar Cells* (Lausanne: EPFL Press) p. 25

[15] Ni J, Zhang J J, Cao Y, Wang X B, Li C, Chen X L, Geng X H and Zhao Y 2011 *Chin. Phys. B* **20** 087309

[16] Zeman M, Willemen J, Vosteen L, Tao G and Metselaar J 1997 *Sol. Energy Mater. Sol. Cells* **46** 81

[17] Vukadinavic M, Smole F, Topic M, Schropp R and Rubinelli F 2004 *J. Appl. Phys.* **96** 7289

[18] Yunaz I, Yamada A and Konagai M 2007 *Jpn. J. Appl. Phys.* **46** 1152

[19] Yunaz I, Sriprapha K, Hiza S, Yamada A and Konagai M 2007 *Jpn. J. Appl. Phys.* **46** 1398

[20] Meillaud F, Shah A, Droz C, Vallat-Sauvain E and Miazza C 2006 *Sol. Energy Mater. Sol. Cells* **90** 2952

[21] Takakura H 1992 *Jpn. J. Appl. Phys.* **31** 2394

[22] Carius R, Folsch J, Lundszien D, Houben L and Finger F 1998 *Mat. Res. Soc. Symp. Proc.* **507** 813

[23] Matsui T, Chang C, Takada T, Isomura M, Fujiwara H and Kondo M 2008 *Appl. Phys. Express* **1** 031501

[24] Rubinelli F, Jimenez R, Rath J and Schropp R 2002 *J. Appl. Phys.* **91** 2409

[25] Zeman M, Willemen J A, Vosteen L L A, Tao G and Metselaar J W 1997 *Sol. Energy Mater. Sol. Cells* **46** 81

[26] Hu Z H, Liao X B, Zeng X B, Xu Y Y, Zhang S B, Diao H W and Kong G L 2003 *Acta Phys. Sin.* **52** 217 (in Chinese)

[27] Kaining D, Thomas K, Bart E P, Carolin U, Alexander M E, Sandra S, Andreas L, Reinhard C and Uwe R 2011 *Sol. Energy Mater. Sol. Cells* **95** 3318

[28] Chang C, Matsui T and Kondo M 2008 *J. Non-Cryst. Solids* **354** 2365